This is the accepted version of the paper.

This version of the publication may differ from the final published version.

(Paper ID: 40) Strain self-sensing tailoring in functionalised carbon nanotubes/epoxy nanocomposites in response to electrical resistance change measurement

Donglan An[a], Jim Nourry[a], Somayeh Gharavian[b], Vijay Kumar Thakur[c], Indrat Aria[d,*], Isidro Durazo-Cardenas[e], Tasnuva Khaleque[f], Hamed Yazdani Nezhad[f,*]

[a]*Enhanced Composites & Structures Centre, Cranfield University, Milton Keynes MK43 0AL, UK*
[b]*School of Materials, The University of Manchester, Oxford Road, Manchester, M13 9PL, UK*
[c]*Department of Engineering, Science and Technology, SRUC, Edinburgh DG1 3NE, UK*
[d]*Surface Engineering Precision Institute, Cranfield University, Milton Keynes MK43 0AL, UK*
[e]*Through-life Engineering Services Centre, Cranfield University, Milton Keynes MK43 0AL, UK*
[f]*Department of Mechanical Engineering & Aeronautics, City University of London, London EC1V 0HB, UK*

Corresponding author. Tel.: +44 20 70405060; *E-mail address:* hamed.yazdani@city.ac.uk

Abstract

Carbon nanotubes (CNTs) are inherently multifunctional, conductive and possess piezo-resistive characteristics. Aiming at the multi-functionality of materials, nanocomposites made of epoxy resin with embedded CNTs are a promising solution for strain self-sensing applications. A critical parameter to achieve repeatable and reliable measure is the CNTs dispersion state in the resin. This study investigated the effect of CNTs concentration (0.01 wt% and 0.1 wt%), with different loading of surfactant Triton X-100, (0.0%, 0.2%, 0.5% and 1.0%) on strain sensing in terms of sensitivity and linearity based on electrical resistance data. The CNTs were synthesised directly using an injection floating catalyst chemical vapor deposition (ICCVD) process and their quality was characterised by Raman spectroscopy and scanning electron microscopy. Only the epoxy modfied with 0.1 wt% CNTs exhibited sufficient piezo-resistivity for the resistance measurements, and those with 0.01 wt% CNTs did not show sufficiently measurable conductivity so were excluded in our study, since their CNTs were highly entangled, and conductive network failed to be established. It was observed that, with 0.1 wt% CNTs, adding 0.5% content of the surfactant improved gauge factor. With more content of the surfactant (1.0 %), surprisingly, we observed a drop of gauge factor by the order of two. Therefore, by comparing the conductivity change between 1.0% and 0.5% surfactant, we postulated that the relatively high content surfactant has reached critical micelle concentration, and negatively affects CNTs dispersion state. The research presented in this article shows that moderate content of surfactant could improve piezo-resistivity gauge factor while excessive surfactant could cause adverse effect.

Keywords: Carbon nanotubes, nanocomposites, piezo-resistivity, self-sensing, in-situ strain measurement, surfactant

1. Introduction

Carbon nanotube (CNTs) based polymer composites are extensively used to improve the electrical conductivity of composites owing to their significantly superior electrical properties [1][2]. CNTs have been investigated for use in various applications due to their superior electrical, thermal, and mechanical properties, which has huge potential to create multi-functional composites [3]–[5]. In addition, CNTs have a large aspect ratio and are chemically stable in a polymer matrix. Consequently, CNTs have been mixed with polymers to fabricate electrically conductive composites [6]–[8]. The cylinder-shaped individual CNTs contact with each other, and form a conductive network in polymers. With more 'contact points' between CNTs, an improved electrical path can be formed [9]. Besides the purity of CNTs, aspect ratio and dispersion state play a critical role on piezo-resistive property. Enhanced conductivity can be achieved with uniformly dispersed CNTs in polymers [10]. Also, it has been reported that the conductivity dramatically improves when CNTs concentration reach the percolation threshold (PT) [11][12]. However, the piezo-resistivity with CNTs above PT has not widely been researched. In the present study, different volume of surfactant was used to create different CNTs dispersion state, and an incremental cyclic tensile testing was conducted, and resistance change was recorded simultaneously.

The aim of this study is to investigate the effect of surfactant on CNTs dispersion state, and furthermore the correlation with the piezo-resistivity for tailoring strain self-sensing. CNTs were

synthesised and characterised using Raman spectroscopy and scanning electron microscopy (SEM) to investigate their dimension and purity. Raman indicated that multi-walled CNTs (MWCNT) possessed minor defects. The SEM images indicated that the CNTs' size was between 20 nm to 100 nm in diameter, and the average length was 40 μm approximately, so the length over length ratio was maximum 2000. Different weight percentages of CNTs, 0.01 wt% and 0.1 wt%, were incorporated with surfactant Triton X-100, which is a non-ionic surfactant. The Triton X-100 surfactant possesses superior property for dispersing CNTs [13]. In the present study, the samples with 0.01 wt% CNTs showed no electrical conductivity, although this concentration is much higher than the reported percolation threshold [14]. This was attributed to the CNTs not achieving a perfect dispersion state in our case, e.g. entangled CNTs failed to establish a conductive path. For the nanocomposite samples containing 0.1 wt% CNTs, 0.5% surfactant resulted in lowest conductivity while 1.0% surfactant showed the highest. Tunnelling resistance also plays an important role in the conductive path, as reported that such resistance is several orders of magnitude higher than contact resistance and CNTs intrinsic resistance [15][16]. Further investigation on the resistance change measurement was carried out. Our study showed that a gauge factor of 0.5% surfactant samples was over three times higher than the samples with 1.0% surfactant, attributed to such tunnelling resistance which caused higher sensitivity than intrinsic resistance change [17] with the evolution of applied strain, suggesting that adding surfactant can tailor the piezo-resistivity of CNTs/epoxy nanocomposites, to attain the highest gauge factor.

2. Materials and methods

2.1. CNTs fabrication

Injection floating catalyst chemical vapor deposition (ICCVD) [18] process was used to produce the nanomaterial, in which a high-temperature resistant glass tube chamber was used as the growing surface. The process details were as follows, see Fig. 2.1:

- Argon gas (1000 sccm) was used as the inert medium flowing in the chamber at atmospheric pressure during the whole process.
- 5.0 wt% ferrocene in toluene was prepared, and after stirring carefully with no visual sediment, the mixture was injected into tube.
- A pre-heater was set as 170℃ on one end of the tube, for gasifying chemicals.
- The temperature of the tube was 750℃. The CNT growth was conducted for 3.5 hrs. before collecting. Approx. 4g of CNTs were produced using this method in one run, see Fig. 2.2.
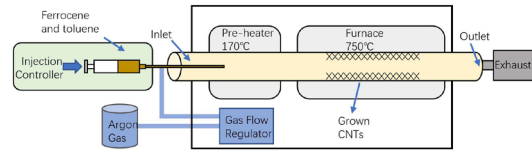

Fig. 2.1. Schematic diagram of ICCVD

2.2. Sample manufacturing

The manufacturing process of the nanocomposite samples was designed to be straightforward, achievable with laboratory chemicals. To fabricate the samples, a mixture of epoxy resin and CNTs was first prepared, was casted into clean glass moulds, and was cured under vacuum conditions to ensure no void or air bubble is trapped. The samples were then cut with a fine bench saw into appropriate size as described below. Finally, the electrical connection and insulation tabs were adhered onto the samples to allow electric resistance measurement and electrical insulation from the test machine, respectively.

To develop the CNTs/epoxy nanocomposite, an aerospace grade epoxy resin system, Araldite 1564 and Aradur 3486 (hardener), was used. Considering the viscosity of the resin (1200 – 1400 mPa.s) and of the hardener (10-20 mPa.s), Acetone (99%) was used to lower the viscosity of the resin system to ease the handling.
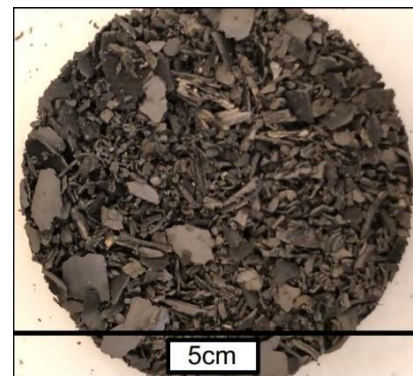

Fig. 2.2. Carbon nanotube flakes as produced by ICCVD

Triton X-100 in aqueous solution was used as a non- ionic surfactant supplied by Sigma-Aldrich. This surfactant was used without further dilution. To prepare the sample for tensile and electrical resistance testing, liquid commercial super-glue was used for adhering testing end tabs; copper conductive tape and RS pro silver paint were used for electrical connection to the surface of the samples, and thick kraft paper was used at the end tabs for insulating test-machine's grips. Several samples were fabricated to investigate the CNTs loading in epoxy, and the effect of surfactant on the dispersion and electrical properties. Table 2.1 shows the details of the different concentration of CNT and surfactant used in this study.

In order to create the nanocomposite samples, a consistent and straightforward method was utilised: First, the CNTs were weighted on laboratory scale under LEV, a certain weight percentage, either 0.1 wt% or 0.01 wt%, were selected relative to the weight of epoxy. The appropriate amount of Triton X-100 was then added into the CNTs and 20 ml of Acetone was poured into the CNTs + TX-100 mixture. Then the mixture was sonicated using a Branson Digital Sonifier probe Sonicator for 15 min, in which the beaker was held in a water bath to prevent the solution from overheating, and the acetone from evaporating, as shown in Fig. 2.3.

Table 2.1. Sample composition details

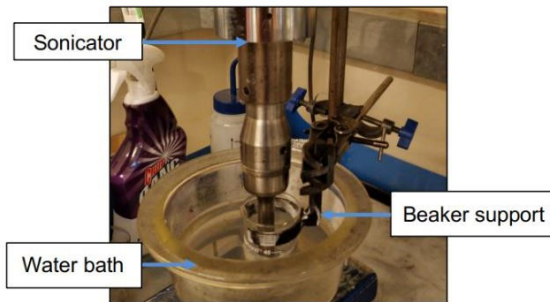| CNTs wt%	Surfactant wt%
0	0
	0
0.01	0.5
	1
	0
	0.2
0.1	0.5
	1

Fig. 2.3. Probe sonicator and water bath setup

Secondly, the CNTs dispersion in acetone was poured into 66.4 g of epoxy resin, hand-mixed to incorporate the acetone to the epoxy to lower its viscosity, and was then sonicated again for 30 min to disperse the CNTs into epoxy resin. This time, the beaker was not held in water and the solution was left to heat up under sonication energy to evaporate the acetone present in the solution.

Then, the dispersion of the CNTs in epoxy was further mixed on a hot plate at 150°C with magnetic stirring at medium speed for 1 hr. This step provided full evaporation of the Acetone and further dispersion of the nanotubes in the resin. The mixture was left to cool down to room temperature before 22g of hardener was added and mixed using magnetic stirring again for 15 min at medium speed. After degassing in vacuum chamber for 45 min until no bubbles were left, the mixtures was poured into a glass mould with a cavity of 80 cm^3 and thickness of 3 mm, as shown in Fig. 2.4. Finally, the mould was placed in a vacuum assisted oven and the resin was cured at 80 °C for 8 hr,

according to the manufacturer's specification for the Araldite + Aradur curing cycle. Four samples were cut out in dimensions of standard tensile test specimens in 150mm × 25mm × 3mm, as shown in Fig. 2.5.
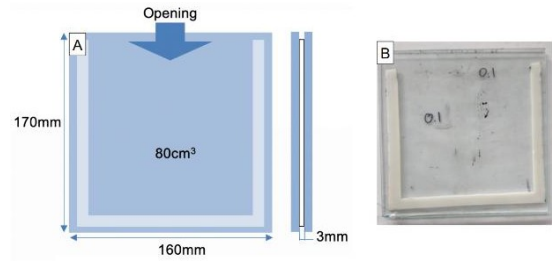

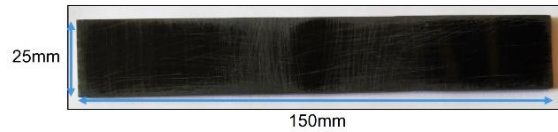Fig. 2.4. Rectangular mould, schematic and actual

Fig. 2.5. Nanocomposite sample after cutting and surface scratch marks for CNTs exposure (thickness = 3mm)

2.3. Tensile and electrical resistance testing

To assess the ability of the CNT-epoxy nanocomposite for strain sensing under tensile deformation, the electrical resistance of the samples was monitored. After cutting the samples, electrodes required for the electrical resistance measurements and the insulated tabs for the tensile machine grips were fabricated. To fabricate the electric connection, each sample was first polished with an abrasive paper with a grain size of 120 in order to scratch the insulating epoxy on surface so the CNTs have been exposed. After washing off the dust with acetone, silver paint was applied to create a 5 mm wide path across the width of the sample, and each path was separated by approximately 40 mm. Finally, copper tape was placed on the fresh silver paint and wrapped three times around the sample. In order to electrically insulate the sample from the grips of the test-machine, thick Kraft paper was used as tabs on the ends of the samples. The paper tabs were approximately 40 mm in length and covered the entire width of the sample, see Fig. 2.6.
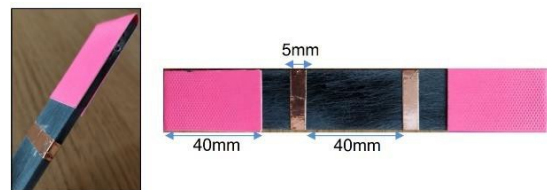

Fig. 2.6. Test samples with tabs and electric connections, copper tape over silver paints

The tensile testing apparatus consisted of the following parts:

- Instron tensile machine + 5KN load + controlling computer_A

- Computer_B running a customized LabView acquisition software
- Data Acquisition (DAQ) system
- Keithley Ohmmeter
- EIR laser extensometer

The Instron tensile machine was linked to the DAQ using BNC cables. The laser extensometer was also connected to the DAQ using a custom- made connection cable phone plug to BNC. The DAQ serve as a gathering point for all the data, it is plugged to Computer_B via USB and is used to input the load, displacement and extension data from the laser into the LabView software which saved and plotted the data. The ohmmeter was also plugged to Computer_B via USB and the electrical resistance data was fed to the LabView software. Crocodile Clips were used to connect the ohmmeter to the test sample, and two reflective targets were placed on the sample to allow measurements of displacements with the laser extensometer. Fig. 2.7 shows the in-situ tensile testing setup and the LabView interface.
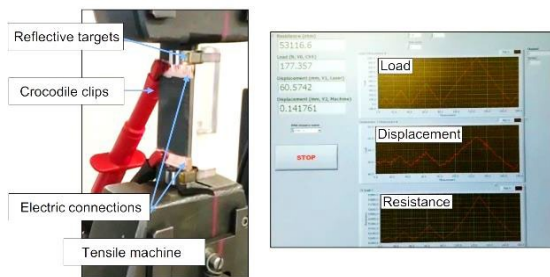

Fig. 2.7. Test sample in the tensile machine and LabView software interface

Based on manufacturer's specification for the resin system, 5 kN load was set before the tensile strength of the cured resin was reached. To test the electrical resistance and observe its evolution during the tensile deformation, a test plan was designed: each sample was loaded in a cyclic manner, the first load was set to 150 N (to ensure elastic deformation) then the load was set back to 0 N, thus the sample would go from 0 N to 150 N then back to 0 N, and this was labelled as the 1st 'loop'. The tensile machine was programmed to perform five loops, from zero load to 150 N, 300 N, 450 N, 1000 N, 2000 N, and unloading back to 0 N after each loop. Conducting such process allowed the investigation of the deformation of the nanocomposites and the electric resistance evolution before the ultimate strength was reached. During testing, the LabView software displayed three curves: Load vs Time, Displacement vs Time and Resistance vs Time.

2.4. Scanning electron microscopy
To investigate the dispersion morphology of the CNTs in the epoxy as well as the aspect ratio of the

CNTs, the LYRA3 TESCAN SEM was utilised. Pieces of each sample were cut from corners and middle regions, polished with 120 grain size abrasive paper, and coated with 20 nm of gold. The pieces were then held on aluminium stubs with conductive carbon tape (gold coat allows an improved conductivity on sample's surface, which leads to better SEM images and the carbon tape was used to discharge the electrons).

2.5. Raman spectroscopy
Raman spectroscopy was performed on the CNTs to further characterise their structure and purification. The nanotubes were dispersed in de-ionized water using probe sonication for 15mins, then one droplet was laid on a silicon substrate with one drop silicon oil. After placing the substrate into Raman spectrometer, the parameters on the machine was set as follows: slit: 300 µm, hole: 400 µm, 10 s acquisition time, five spectrums. A 632.81 nm wavelength red laser at 100% power and X100 objective was used.

3. Results and discussion

The main aspect of this research is to assess the strain sensing ability of the functionalised CNTs/epoxy nanocomposite at different level of functionalisation using the surfactant which manipulates the quality of the material bonds at molecular scale. The morphological characteristics of the CNTs were assessed, such as their length and diameter. The chemical characteristics of the CNTs were also determined, e.g. purity which directly results in the capability of the nanocomposites for strain sensing. It may be noteworthy that aiming at the perfect single-walled nanotube does not always lead to the best sensing outcome; it is the matter of finding the right characteristics that would fit the application, herein strain sensing in laboratory scale.

3.1. Carbon nanotubes characterization
Fig. 3.1 shows the SEM image of a CNT bundle, without functionalisation treatment/surfactant. The diameter measured was between 20 nm and 100 nm, and the length was approximated to be 40 µm. The investigation also indicated the presence
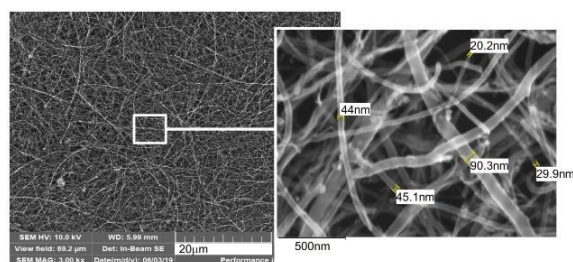

Fig. 3.1. Scanning electron microscopy image of pristine CNTs bundle

of MWCNTs. In this case, the SEM image suggests a higher number of walls in the CNTs structure.

The length and diameter of the nanotubes are directly related to their synthesis process. The temperature of the furnace (750°C) as well as the rate of flow of ferrocene in the chamber and the growth time, all have been reported to affect the morphology of the CNTs [19], suggesting that finer tuning of the synthesis parameters can be applied to increase the uniformity of the CNTs or lower their diameter. However, the length and diameter observed on the SEM images are consistent with the literature [20] though the inner diameter of the tubes was not investigated in the present work due to the scale of the strain sensing investigations.

Generally, MWCNTs with large diameter are preferable for strain sensing application due to the improved strain transfer between the resin and the nanotubes, repeatability and linearity of the measurements [21]. Furthermore, their electrical conductivity remains comparable to the SWCNTs because most of the electrons are travelling between the layers of the nanotubes [22][23].

To further characterise the type of nanotubes, Raman spectroscopy was performed. Fig. 3.2 shows the Raman spectrum of dried CNT on a silicon substrate along with the important peaks relevant to CNTs identification.

Four major bands were present for the CNTs in the spectrum, the Radial Breathing Mode (RBM) band at 110 cm^{-1}, D band at 1320 cm^{-1}, G band at 1575 cm^{-1} and G´ band at 2650 cm^{-1}. The RBM band corresponds to the in-phase movement of all carbon atoms in the radial direction [24]. The D band is related to disturbance in the hexagonal graphitic structure, and it is often an evidence of amorphous face or impurity of the nanotubes [25]. The 3rd peak, the G band, is directly related to the graphitic structure, and relates to the movement of neighbouring atoms in opposite direction. Lastly, the G´ band which is a second order harmonic of the D band is representative of a self-annealing pair of phonons and can occur in defect-free nanotubes.
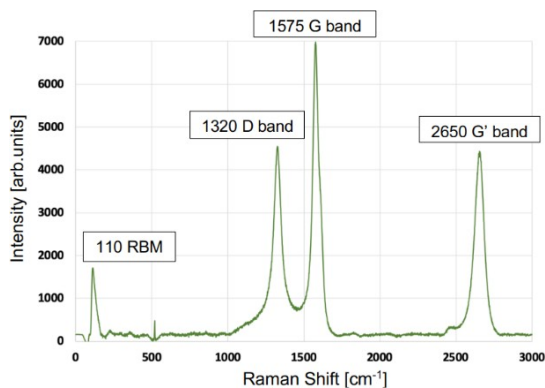
Fig. 3.3 shows a schematic of atoms movement leading to RBM and G bands.

The RBM band at 110 cm^{-1} is clearly visible and of good intensity (See Fig. 3.2). It was reported that the RMB band of single walled nanotube is observable with good intensity whereas the RMB band of MWCNT is low in intensity and difficult to see [26][27]. This effect is due to the damping of movement of atoms due to multiple wall movements inside the tubes. The RBM band is linked to the nanotube diameter given by

$$\omega_{RBM} = \frac{A}{d} + B \qquad (1)$$

where d is the diameter of the tube, A and B are constants related to the surroundings of the nanotube. Dresselhaus et al. suggested the value of $A = 248$ and B can be neglected [28]. In the present study, the diameter 2.25 nm, of the nanotube was determined using equation 1. This approximation may apply more accurately to single-walled CNTs but provided an idea of the number of CNTs' walls in the present study. To access the quality and the abundance of graphitic structure, the ratio between the intensity of the G and D band is often considered. In the present study, the intensity of the D band is close to the intensity of the G band, which suggests high defect and amorphous phase in the CNT but it is also a good indicator of the presence of MWCNTs. The multiple inner walls of the tubes are prone to defects. By increasing the number of inner tubes and creating MWCNTs the probability of having defects increases, explaining the intensity of the D band.
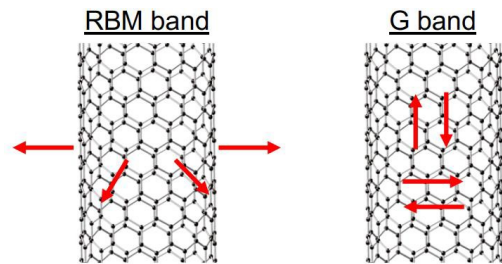

Fig. 3.3. Schematic of atom movements for RBM and G bands

Another feature of the G band is its shape in the spectrum, as seen thin and sharp. Such shape can be linked to the electrical properties of the nanotube, whether they are metallic or semi-conductive. In our case, the shape of the G band is close to the shape of a Highly Oriented Pyrolytic Graphite (HOPG) as mentioned in the literature [27]. Although, the high intensity of the peak would suggest a semi-conductive type of nanotube, further investigation is needed to draw a full picture on it.

The simultaneous qualitative analysis of the Raman spectrum and the SEM images led to the conclusion that the nanotubes are multi-walled with large numbers of walls with relatively higher conductivity than single-walled ones.

Fig. 3.2. Raman spectrum of dry Carbon nanotubes on Silicon substrate

Their purity and amount of crystalline graphene structure is still to be precisely determined along with a thorough investigation of peak position.

3.2. Carbon nanotube dispersion

In order to understand the electrical behaviour of the nanocomposite, the dispersion of the nanotube was characterised. First, a visual characterisation was performed. Each sample was placed on a backlit surface, the epoxy resin being transparent and the nanotubes being black. The images provided a good first look at the CNTs distribution, as shown in Fig. 3.4.
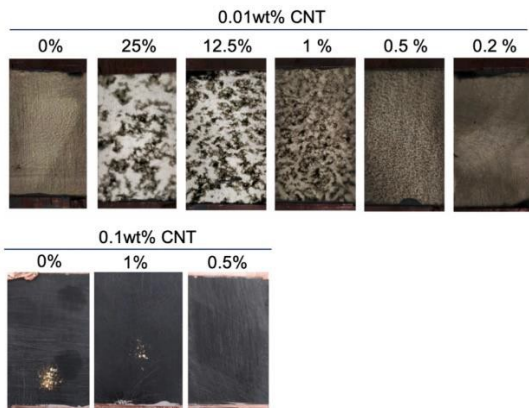

Fig. 3.4. Picture of backlit sample for 0.01wt% CNT and 0.1wt% CNT, with different surfactant concentration

Each group (0.1 wt% CNTs modified epoxy and 0.01 wt% CNTs modified epoxy) can be easily distinguished, thanks to their opacity. The 0.1 wt% CNTs modified epoxy was the only conductive one, which means that in the 0.01 wt% CNTs group, the dispersion of nanotubes did not reach the percolation threshold to create a conductive network within the material. Agglomeration is evident in the 0.01wt% group. However, with the addition of 1% surfactant the CNTs began to disperse and cover more space. When 0.5% surfactant is added, the sample becomes fully opaque showing a relatively better dispersion.

The sample with 0.2% surfactant presents a continuous grey colour without visible agglomeration, see Fig. 3.4. At this concentration, the surfactant is supposedly under its critical micelle concentration (CMC) and did not form long micelles but surrounded and dispersed the nanotubes [29]. It is not possible to know precisely the 3-dimensional distribution of the CNTs in the material, especially within the conductive group with 0.1 wt% CNTs. To have a better understanding of the dispersion inside the material, pieces of each sample were observed with the SEM. The purpose was to examine the cross- sectional area of the material but depending on where the SEM samples were cut on the original samples it was difficult to see the CNTs in the resin.

Fig. 3.5 shows SEM image of the 0.1wt% CNTs modified epoxy sample with 1% Tx-100.
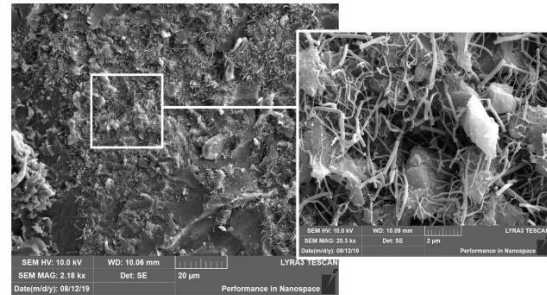

Fig. 3.5. Scanning Electron Microscopy Image of Carbon Nanotubes dispersion in epoxy resin, 0.1wt% CNT + 1% Tx-100

It is evident that the CNTs have been shorten by the nanocomposite fabrication process, due to the continuous use of probe sonication for 45 min during the mixing stage. They have not been observed as highly entangled; probably due to their short length and the extensive area well covered by the CNTs. However, this image shown in Fig. 3.5 was taken at an area with densely populated CNTs.

3.3. Tensile tests and resistance measurements

Electrical conductivity was overserved in 0.1 wt% CTNs modified epoxy during the tensile test. The evolution of the electrical resistance during the tensile testing was obtained and compared for different concentration of surfactant. The gauge factor was also calculated as an indication of sensor performance.

Fig. 3.6(a) shows the change of the electrical resistance when tensile strain is applied. Each cycle (1 to 5) is shown along with the load level. The starting resistance of the 0.1 wt% CNTs modified epoxy with no surfactant was 20 ± 5 kW. The tensile strain was observed in the elastic region of the material for the first three cycles, before plastic deformation was induced, at which zero strain is not recovered after unloading to zero after the 4th cycle. Also, the resistance change followed the strain during the first three cycles but during the 4th and 5th cycles the resistance change was significantly higher than that of the strain. This is observed in the increasing gauge factor throughout the test, which the resistance does not change linearly with strain evolution. Moreover, the maximum change of resistance was of approximatively 4% of the original value for a strain of 2%.

Fig. 3.6(b) shows the change of resistance and strain versus time for 0.1 wt% CNTs with 0.5% Tx-100. With the addition of 0.5% of surfactant (Tx-100), the curve changed drastically. The resistance did not change linearly with strain and the gauge factor

increases throughout the test as was observed in the case of no surfactant. However, it is observed that with the same level of plastic deformation induced in the material, the resistance response is 100% higher than that without the surfactant. A 2% strain change in strain caused an 8% change in electrical resistance. The sensitivity seems to be improved, but the starting resistance of this sample was 3.5 ± 0.1 MW.
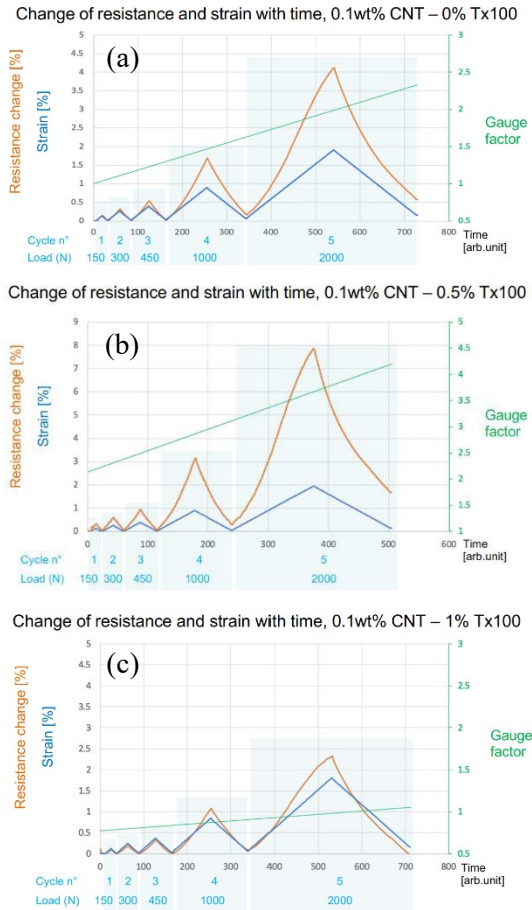

Fig. 3.6. Curve of Resistance change and Strain versus Time for (a) 0.1wt% CNT and no surfactant, (b) 0.1wt% CNTs and 0.5% Tx-100, and (c) 0.1wt% CNT and 1% Tx-100

With further increase of the surfactant concentration to 1% Tx-100, the materials properties seem to stabilize. Fig. 3.6(c) shows the change of resistance and strain versus time for 0.1wt% CNT modified epoxy with 1% Tx-100. The gauge factor increases but much slower than that with no surfactant or with 0.5% surfactant and evaluated, approximately, between 0.75 and 1. The resistance started at 10 ± 1 kW. It is the highest conductivity reached among all the samples. Although, the sensitivity was lower, the resistance change followed the strain trend in a semi-linear manner, reaching approximatively 2.5% change when strain reached 1.75%.

3.4. Mechanical properties

Fig. 3.7 shows the Load vs Displacement curves of the conductive samples (0.1wt% CNT) for each concentration of surfactant in comparison with the unmodified epoxy. Fig. 3.7 A shows that the curves match each other, indicating no change in mechanical properties. However, when 0.5% TX-100 is added, the nanocomposite weakened and showed more strain at the same load level. With the addition of 1% TX-100, the mechanical properties slightly improved.

With the addition of 0.5% TX-100 the critical micelle concentration was reached, and the surfactant facilitated the fine dispersion of the CNTs in the matrix. Due to inherent discontinuity in stress transfer from the resin to the CNTs in cases with no functionalisation, the nanotubes acted like defect sites and weakened the epoxy. On the other hand, when the concentration of surfactant is above the CMC, e.g. for 1% TX-100, the CNTs are fully surrounded by surfactant micelles. These micelles improve bonding quality between the epoxy and the CNTs, and thus improving the load transfer which enhances strengthening of the epoxy.

3.5. Effect of adding surfactant

The purpose of adding surfactant before the mixing stage is to aid the dispersion of nanotubes by unravelling the bundles. The measured electrical resistance of the nanocomposite was approximately 3.5MΩ with the addition of 0.5% surfactant, which was the highest resistance measured among all the samples. This indicates that the surfactant facilitated the dispersion of the nanotubes and unravel the bundles. However, good dispersion of CNTs was observed with the addition of 1% surfactant. For example, a matrix where every single nanotubes are separated from its neighbour will exhibit an extra fine dispersion but a high resistance, because electrons will be able to travel only through tunnelling effect rather than contact points, as was observed for 0.1 wt% CNTs modified epoxy with 0.5% TX100, see Fig. 3.6(b). The dispersion was too fine to achieve good conductivity hence a high resistance was obtained. Moreover, since the dispersion was extra fine and the electrons were travelling through tunnelling effect, the sensitivity of the sensor was greater than any other sample. The tunnelling conductivity decreases exponentially with the distance between the CNTs, therefore a little change in CNTs distance can contribute to a large change in tunnelling resistance, hence the large increase in gauge factor with the evolution of applied strain.

For 0.1 wt% CNTs modified epoxy with 1% Tx100, the resistance was approx. 10 kΩ , the lowest resistance reached among all samples, see Fig. 3.6(c). This is due to the fact that the surfactant is above its CMC and started to agglomerate the CNTs. The conductive network of CNTs is denser, with more nanotubes contacting each other. This would explain the more linear behaviour of the resistance change when strain was applied.

Finally, though the original idea was to achieve a well dispersion of CNTs, the results suggest that some level of agglomeration is desirable for the linearity of the measurement, to have a detectable resistance while using a low weight percentage of CNTs. The other strategy would be to seek the best dispersion possible and increase the CNTs loading to reach better level of conductivity and linearity.

4. Conclusion

The mechanical properties of the epoxy resin was improved with the addition of the CNTs, only when 1% surfactant was added to the composition. The percolation threshold was observed for the samples modified with 0.1 wt% CNTs whereas samples modified with 0.01wt% CNTs were not conductive.

This work aimed to investigate the performance of CNTs/epoxy nanocomposites for strain sensing through electrical resistance measurement, with the addition of varying weight percentages of CNTs and surfactant Triton X-100. Using ICCVD, it was possible to synthesise MWCNTs with D and G bands, sufficiently conductive to use in fabrication of CNTs/epoxy nanocomposites which were able to sense tensile deformation through electrical resistance change measurements.

The effect of non-ionic surfactant, Trion X-100, was investigated and the concentration of 0.5% and 1% with 0.1wt% CNTs in epoxy was found to yield the best results in terms of linearity of gauge factor and electrical conductivity. The addition of 0.5% surfactant resulted in a higher gauge factor and the addition of 1.0% surfactant significantly increased the electrical conductivity. The resistance change was mainly due to the increasing distance between the CNTs because of applied strain evolution. This directly affects the ability of the electron to hop from the edge of one nanotube to another which increased the resistance of the sample enabling the strain measurement. In terms of conductivity, improving the dispersion to a perfect state with all CNTs detached from each other is not always desirable as it can lower the electrical conductivity of the samples especially for small CNTs content. Therefore, from our research it was found that when CNTs content is moderate, a semi-uniform

dispersion state is preferable to establish an effective electrical conductivity, depending on the pattern of the CNTs network, while the higher piezo-resistivity can be achieved with well-dispersed CNTs, from which tunnelling resistance plays an more important role and it is more sensitive to applied strain.
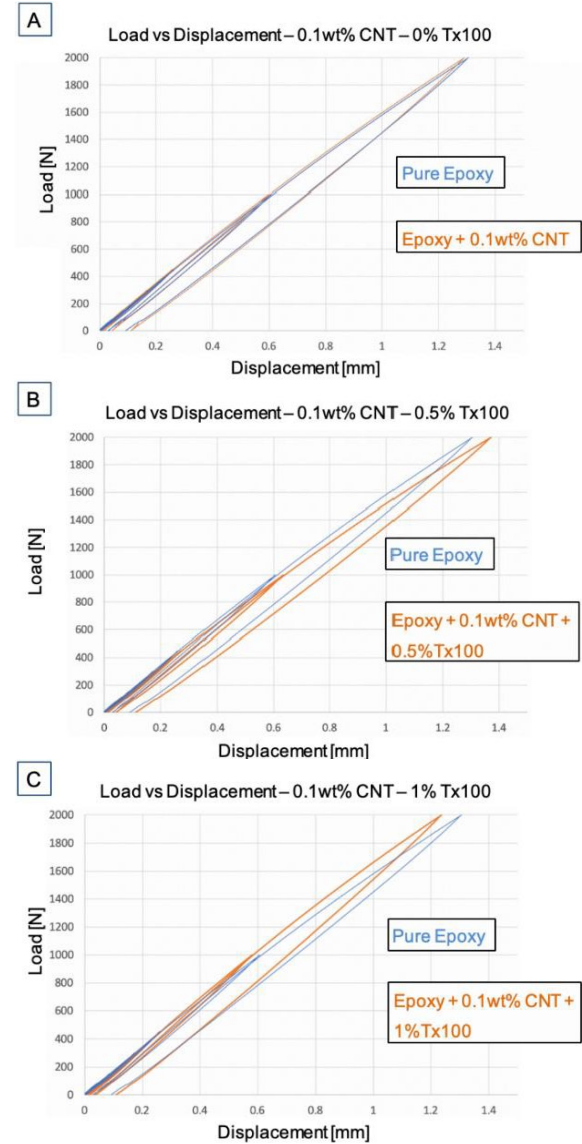

Fig. 3.7. Load versus Displacement curves for pure Epoxy and Epoxy + 0.1wt% CNTs with A) no surfactant B) 0.5% Tx100 C) 1% Tx100

References

[1] A. I. Medalia, "Electrical Conduction in Carbon Black Composites.," Rubber Chemistry and Technology, vol. 59, no. 3. pp. 432–454, 1986.

[2] H. Babaei, P. Keblinski, and J. M. Khodadadi, "Improvement in thermal conductivity of paraffin by adding high aspect-ratio carbon-based nano-fillers," Phys. Lett. Sect. A Gen. At. Solid State Phys., vol. 377, no. 19–20, pp. 1358–1361, 2013.

[3] K. Chu, D. Kim, Y. Sohn, S. Lee, C. Moon, and S. Park, "Electrical and thermal properties of carbon-nanotube composite for flexible electric heating-unit applications," IEEE Electron Device Lett., vol. 34, no. 5, pp. 668–670, 2013.

[4] S. K. Hong, D. Kim, S. Lee, B. W. Kim, P. Theilmann, and S. H. Park, "Enhanced thermal and mechanical properties of

carbon nanotube composites through the use of functionalized CNT-reactive polymer linkages and three-roll milling," Compos. Part A Appl. Sci. Manuf., vol. 77, pp. 142–146, 2015.

[5] J. Alam, A. Khan, M. Alam, and R. Mohan, "Electroactive shape memory property of a Cu-decorated CNT dispersed PLA/ESO nanocomposite," Materials (Basel)., vol. 8, no. 9, pp. 6391–6400, 2015.

[6] K. Chu, S. C. Lee, S. Lee, D. Kim, C. Moon, and S. H. Park, "Smart conducting polymer composites having zero temperature coefficient of resistance," Nanoscale, vol. 7, no. 2, pp. 471–478, 2015.

[7] C. Min, X. Shen, Z. Shi, L. Chen, and Z. Xu, "The electrical properties and conducting mechanisms of carbon nanotube/polymer nanocomposites: A review," Polym. - Plast. Technol. Eng., vol. 49, no. 12, pp. 1172–1181, 2010.

[8] B. Fiedler and K. Schulte, "Carbon nanotube-based composites," Compr. Compos. Mater. II, vol. 4, no. 1, pp. 201–229, 2017.

[9] S. Pfeifer, S. H. Park, and P. R. Bandaru, "Analysis of electrical percolation thresholds in carbon nanotube networks using the Weibull probability distribution," J. Appl. Phys., vol. 108, no. 2, 2010.

[10] L. Arronche, V. La Saponara, and S. Yesil, "Impact Damage Sensing of Multiscale Composites Through Epoxy Matrix Containing Carbon Nanotubes," pp. 2797–2806, 2013.

[11] W. Bauhofer and J. Z. Kovacs, "A review and analysis of electrical percolation in carbon nanotube polymer composites," Compos. Sci. Technol., vol. 69, no. 10, pp. 1486–1498, Aug. 2009.

[12] Y. Geng, M. Y. Liu, J. Li, X. M. Shi, and J. K. Kim, "Effects of surfactant treatment on mechanical and electrical properties of CNT/epoxy nanocomposites," Compos. Part A Appl. Sci. Manuf., vol. 39, no. 12, pp. 1876–1883, Dec. 2008.

[13] J. Njuguna, O. A. Vanli, and R. Liang, "A Review of Spectral Methods for Dispersion Characterization of Carbon Nanotubes in Aqueous Suspensions," J. Spectrosc., vol. 2015, pp. 1–11, Jun. 2015.

[14] X. Zeng et al., "Characteristics of the electrical percolation in carbon nanotubes/polymer nanocomposites," J. Phys. Chem. C, vol. 115, no. 44, pp. 21685–21690, 2011.

[15] W. S. Bao, S. A. Meguid, Z. H. Zhu, and G. J. Weng, "Tunneling resistance and its effect on the electrical conductivity of carbon nanotube nanocomposites," J. Appl. Phys., vol. 111, no. 9, 2012.

[16] Y. Yu, G. Song, and L. Sun, "Determinant role of tunneling resistance in electrical conductivity of polymer composites reinforced by well dispersed carbon nanotubes," J. Appl. Phys., vol. 108, no. 8, 2010.

[17] W. Obitayo and T. Liu, "A review: Carbon nanotube-based piezoresistive strain sensors," J. Sensors, vol. 2012, 2012.

[18] O. Guellati et al., "CNTs' array growth using the floating catalyst-CVD method over different substrates and varying hydrogen supply," Mater. Sci. Eng. B Solid-State Mater. Adv. Technol., vol. 231, no. August 2017, pp. 11–17, 2018.

[19] Q. Zhang, J. Liu, R. Sager, L. Dai, and J. Baur, "Hierarchical composites of carbon nanotubes on carbon fiber: Influence of growth condition on fiber tensile properties," Compos. Sci. Technol., vol. 69, no. 5, pp. 594–601, 2009.

[20] C. Singh, M. S. P. Shaffer, and A. H. Windle, "Production of controlled architectures of aligned carbon nanotubes by an injection chemical vapour deposition method," Carbon N. Y., vol. 41, no. 2, pp. 359–368, 2003.

[21] I. Kang, M. J. Schulz, J. H. Kim, V. Shanov, and D. Shi, "A carbon nanotube strain sensor for structural health monitoring," Smart Mater. Struct., vol. 15, no. 3, pp. 737–748, 2006.

[22] S. Frank, P. Poncharal, Z. L. Wang, and W. A. De Heer, "Carbon nanotube quantum resistors," Science (80-.)., vol. 280, no. 5370, pp. 1744–1746, 1998.

[23] A. Bachtold et al., "Aharonov-Bohm oscillations in carbon nanotubes," Nature, vol. 397, no. 6721, pp. 673–675, 1999.

[24] R. Saito, M. Hofmann, G. Dresselhaus, A. Jorio, and M. S. Dresselhaus, "Raman spectroscopy of graphene and carbon nanotubes," Adv. Phys., vol. 60, no. 3, pp. 413–550, 2011.

[25] M. Sveningsson et al., "Raman spectroscopy and field-emission properties of CVD-grown carbon-nanotube films," Appl. Phys. A Mater. Sci. Process., vol. 73, no. 4, pp. 409–418, 2001.

[26] J. M. Benoit, J. P. Buisson, O. Chauvet, C. Godon, and S. Lefrant, "Low-frequency Raman studies of multiwalled carbon nanotubes: Experiments and theory," Phys. Rev. B - Condens. Matter Mater. Phys., vol. 66, no. 7, pp. 1–4, 2002.

[27] M. S. Dresselhaus, G. Dresselhaus, and A. Jorio, "Raman spectroscopy of carbon nanotubes in 1997 and 2007," J. Phys. Chem. C, vol. 111, no. 48, pp. 17887–17893, 2007.

[28] M. S. Dresselhaus, G. Dresselhaus, A. Jorio, A. G. Souza Filho, and R. Saito, "Raman spectroscopy on isolated single wall carbon nanotubes," Carbon N. Y., vol. 40, no. 12, pp. 2043–2061, 2002.

[29] A. Vishnyakov, M. T. Lee, and A. V. Neimark, "Prediction of the critical micelle concentration of nonionic surfactants by dissipative particle dynamics simulations," J. Phys. Chem. Lett., vol. 4, no. 5, pp. 797–802, 2013.